16th International Heat Pipe Conference (16th IHPC)
Lyon, France, May 20-24, 2012

Simulation of Heat Transfer in Liquid Plugs Moving Inside Dry Capillary Tubes

Ashish Kumar Bajpai and Sameer Khandekar*
Department of Mechanical Engineering
Indian Institute of Technology Kanpur, Kanpur 208016, India
*E-mail: samkhan@iitk.ac.in

ABSTRACT

The present work numerically simulates the flow of a single isolated liquid plug (of glycerine and water, respectively) flowing in a round capillary tube (ID = 2.0 mm), to understand its local thermal transport behavior. When an isolated liquid plug moves in a capillary tube there is a difference in the advancing and receding dynamic contact angles of the two menisci, respectively. This has been considered in the simulations. The linearized simplification of Hoffman-Tanner's law is used to model the variation in the two respective apparent contact angles, with the velocity of the liquid plug (i.e. $Ca = \mu U/\sigma$). Simulations are carried out for a range of Capillary number and length of liquid plugs. It has been found that variation in dynamic contact angle leads to enhanced local and average heat transfer coefficient in the moving liquid plug; the local fluid circulation being affected by meniscus deformations. In addition, as the length of the liquid plug is increased, heat transfer coefficient decreases and finally shows the asymptotic transport behavior of Poiseuille flow. Other than Capillary number, the fluid Prandtl number strongly affects the local thermo-hydrodynamics.

KEY WORDS: Taylor bubble flow, contact angle hysteresis, plug flow, capillary tube, transport coefficients

1. INTRODUCTION

Micro-scale two-phase flow is an active research area because of its application in many engineering devices like microreactors, catalyst coating in capillaries, electronics cooling, refrigeration industry, flow in blood vessels, porous media etc. [Gunther et al. (2004), Kolb et al. (1991), Zheng et al. (2007)]. Taylor flow or slug flow, characterized by long bubble slugs separated by liquid plugs, constitutes the typical regime under such conditions. Many researchers have worked in the Taylor flow regime [Triplett et al. (1999), Zhao et al. (2001)] and tried to understand the thermo-hydrodynamic properties of such flows. A recent review of local hydrodynamics in such flows, especially in the context of pulsating heat pipes, can be found in Khandekar et al. (2010). Internal circulations in liquid plug have been found to be the major cause of enhanced heat (and/or mass) transfer in such flows. However, not many studies have reported the impact of the dynamic local meniscus level deformations due to the imposed plug velocity on local plug transport behavior.

When a small liquid plug flows in a small diameter tube ($Bo < 2$), the capillary forces play a major role and gravity become relatively insignificant. In such a case, the interfacial tension between solid-liquid (σ_{SL}) and solid-gas (σ_{SG}) should also be taken into account during analysis; surface wettability of the tube wall becomes a critical factor in determining the flow behavior. A single moving liquid plug inside a capillary tube is enclosed by two menisci. During its motion, the dynamic contact angle formed between the flowing liquid meniscus and the solid surface is achieved by a balance between the capillary and the viscous forces. Thus, the moving menisci of the liquid plug are characterized by advancing and receding contact angles, which are different from the static contact angle because of the interplay between surface tension and viscous forces. The relative scaling of these two forces is represented by the Capillary number ($Ca = \mu U/\sigma$). Rose and Heins (1962) were amongst the first to highligh the relation between the advancing contact angle and average velocity U of three-phase contact line. Later on, various researchers like Hoffman (1974), Tanner (1991) and Blake (2006) studied the wetting behavior and dependency of the advancing contact angle on Ca and the static contact angle. Researchers like Barajas et al. (1992), Lee et al. (2008), Walsh et al. (2011) have tried to analyze the surface wettability and heat transfer but none of them incorporated the real dynamic interface. Tripathi et al. (2010) and Shekhawat et al. (2009) previously tried to experimentally understand such phenomenon in oscillating contact line motion in a square capillary tube and presented the hydrodynamics of oscillating meniscus. This work is an attempt to analyze the heat transfer in isolated Taylor bubble flow by including the contact angle hysteresis.

Glycerine and water have been chosen to get a range of Prandtl number and static wettability characteristics. Further, Taylor flow conditions can occur either as (i) wet plug flow regime where a liquid thin film exists at the wall around the bubble (pre-wetted capillary) and (ii) dry plug flow regime where no such film exists. We focus only on the latter case while the former is intended for future scrutiny.

2. PROBLEM FORMULATION

2.1 Physical description

A liquid plug of length L is moving inside a previously dry capillary tube of inner diameter D with a constant velocity U. It is subjected to either a constant temperature or a constant heat flux boundary condition at the tube wall. Because of low Bond number ($Bo < 2$), gravity effect is negligible and surface tension plays an important role in determining the thermo-hydrodynamic behavior of the plug. Figure 1 explains the physical problem under consideration, where θ_s is the static contact angle and θ_a and θ_r are the advancing and receding contact angles of the interface respectively, when liquid plug moves with velocity U.

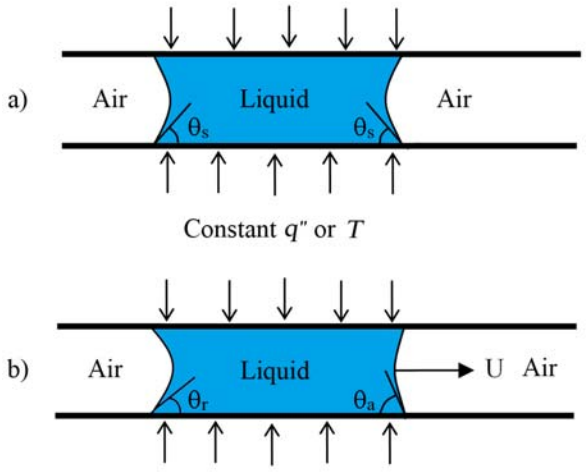

Figure 1: Problem description (a) static plug where θ_s is static contact angle (b) moving plug, where θ_a is the advancing and θ_r is the receding contact angle

2.2 Modeling of dynamic contact angles

Modified Hoffman-Tanner's law is used to determine the dynamic contact angles. According to this law, dynamic contact angle is given as [Berthier (2008)]:

$$\theta_d^3 - \theta_s^3 = ACa \qquad (1)$$

where, θ_d and θ_s are dynamic and static contact angles respectively, Ca is Capillary number and A is a constant whose value is approximately equal to 94 when angles are taken in radians. Berthier (2008) further simplified this model and linearized Eq. (1) by series expansion, under the assumption of small Capillary number (~ Ca < 0.1). Hence, the dynamic advancing and receding contact angles (θ_a and θ_r respectively) are given as:

$$\theta_a = \theta_s + \frac{A|Ca|}{3\theta_s^2} \qquad (2a)$$

$$\theta_r = \theta_s - \frac{A|Ca|}{3\theta_s^2} \qquad (2b)$$

2.3 Governing equations

The governing transport equations i.e. continuity, momentum and energy equations for a Newtonian incompressible fluid with constant properties respectively, can be written as:

$$\nabla \cdot \vec{V} = 0 \qquad (3)$$

$$\rho \frac{D\vec{V}}{Dt} = -\nabla p + \mu \nabla^2 \vec{V} \qquad (4)$$

$$\rho C_p \frac{DT}{Dt} = k \nabla^2 T \qquad (5)$$

Nusselt number, Nu, is defined as

$$Nu = \frac{hL_c}{k} \qquad (6)$$

where, D is the diameter of the tube. The heat transfer coefficient h is given by:

$$h = \frac{q''}{(T_w - T_{avg})} \qquad (7)$$

where, q'' is the heat flux at the wall, T_w is the wall temperature and T_{avg} is the local mean temperature of the fluid in the plane perpendicular to the wall. In case of constant heat flux, q'' is known to us, T_{avg} and T_w is obtained from the solution data at the wall. In case of constant temperature boundary condition, T_w is known, and T_{avg} and the ensuing heat flux are obtained from the solution. Average Nusselt number along the length of the plug is then given by (see Figure 2 for axes index):

$$Nu_{avg} = \frac{1}{L}\int_0^L Nu_x dx \qquad (8)$$

2.4 Numerical method

Lagrangian approach of moving frame is used to analyze the heat transfer and simulate the flow with moving walls, while keeping the plug stationary. The circular wall is given a velocity in the negative X direction while the plug is at rest, as shown in Figure 2. Symmetric boundary condition is used at plane Z = 0 while no slip boundary condition is used at the wall. The interface is simulated with zero heat flux and zero shear stress i.e. free surface boundary condition. Both, constant heat flux ($q'' = 10{,}000$ W/m^2) and constant temperature boundary conditions ($T_w = 350$ K) at the wall, have been solved, respectively. Initial temperature of the fluid is taken to be 300 K; fluid properties are kept constant. Table 1 gives the range of parameters used for the study. Geometry and mesh is created using Gambit®-2.3 with unstructured tetrahedral elements. The model is solved using unsteady pressure based solver in Ansys-Fluent®-v12.0 for water and glycerin, thus giving a wide range of Prandtl Number and surface wettability conditions. PISO algorithm is used for pressure-velocity coupling while the PRESTO interpolation is used for computing the face pressure. Momentum and energy equations are descretized using a second-order upwind scheme for better accuracy while temporal discretization is done using second-order implicit scheme. Green-Gauss node-based averaging scheme is used to evaluate gradients and derivatives as recommended by the Fluent® manual [Ansys Fluent® manual].

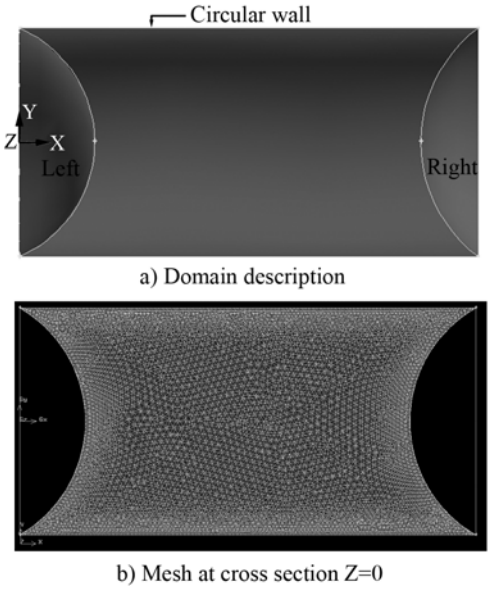

Figure 2: (a) Domain description and, (b) mesh at symmetric plane for a glycerin plug of L/D = 2 at Ca = 10^{-3}, finer mesh near interfaces and coarser in center

Table 1: Range of parameters

Fluid	Ca	Pr	Re_D	Bo
Water	10^{-5} to 10^{-3}	3.56	1.42-142	0.737
Glycerine		6780	2.5 X 10^{-6} - 2.5 X 10^{-4}	0.883

3. PROCEDURE

3.1 Experimental investigation of contact angle

To determine the initial static contact angle of the working fluids, water and glycerin are carefully introduced in dry capillary tubes so as to produce isolated single plugs, respectively. The capillary tubes are made of Pyrex glass of inner diameter 2.0 mm and are thoroughly cleaned and rinsed before the experiment. Images are captured using high resolution digital camera fitted with a macro lens. Figure 3 shows the captured liquid plug images, with respective static contact angle for water and glycerin plugs. Hence, average static contact angle for water is taken to be 67° and that for glycerin is taken to be 30°.

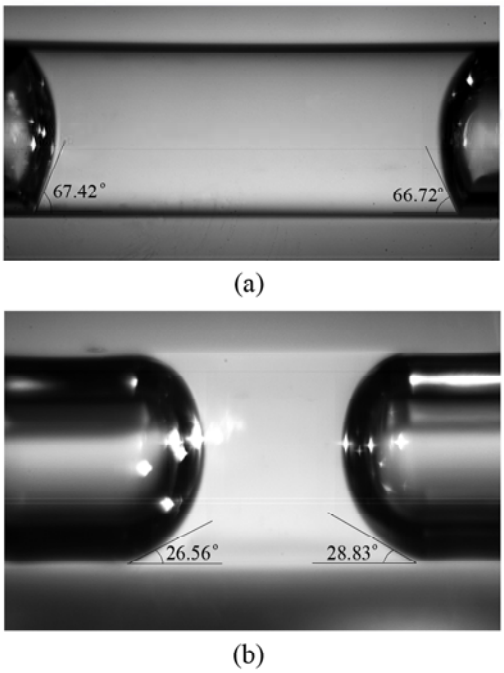

Figure 3: Captured images of liquid plug of (a) water and (b) glycerin in the capillary tube (ID = 2.0 mm)

3.2 Numerical simulations

Numerical simulations are carried out using the technique described above for different *L/D* ratios of the liquid plugs, i.e., *L/D* = 1, 2 and 4 and for different Capillary numbers, i.e., *Ca* = 10^{-5}, 10^{-4} and 10^{-3} for water and glycerin liquid plugs. Grid independence test is carried out for four different

grid element sizes at $Ca = 10^{-3}$ and $L/D = 2$, taking glycerin as the working fluid. Figure 4 (a) and (b) show the grid independence and validation test, respectively. In Figure 4(a), non-dimensional centerline velocity is plotted against the distance from entrance. It is clear that the numerical results are independent of grid after starting element size 0.04. Hence, all other simulations are carried out taking this as the initial smallest element size. To validate the present model, a test is carried out against fully developed Poiseuille flow. Figure 4(b) shows the results for this simulation. The maximum error between the theoretical results and simulation results is 0.05% at the point of maximum velocity which is satisfactory.

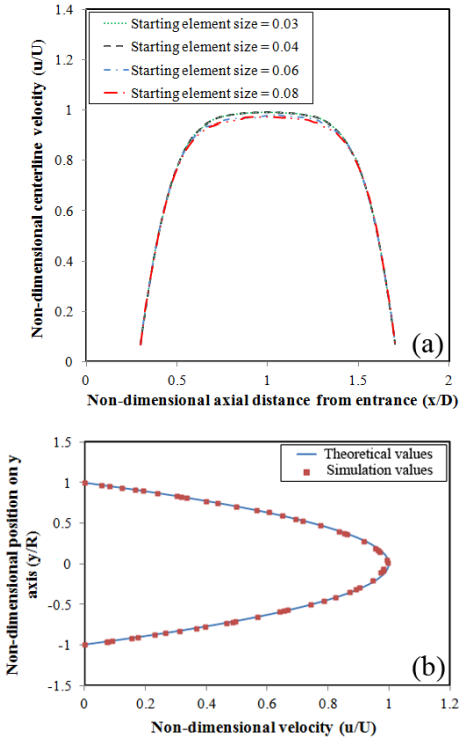

Figure 4: (a) Grid independence test for glycerin plug at L/D = 2 and Ca=10^{-3} and (b) validation test against fully developed Poiseuille flow

4. RESULTS AND DISCUSSION

Figure 5 shows the temporal variation of average Nusselt number (averaged over the length of plug) for glycerin and water plug with L/D = 2.0, $Ca = 10^{-3}$ and constant heat flux boundary condition. The re-circulation time scale $(D+2L_s)/U$ is used to define non-dimensional time scale. Two separate cases are reported for comparison (i) taking dynamic contact angle variations, as per Eq. 2 and, (ii) fixed contact angles, equal to the respective static contact angles, irrespective of the plug velocity.

Several important aspects are noted from Figure 5. Firstly, steady state Nu_{avg} is attained very early in the case of glycerin plug. Another notable feature is the initial fluctuations observed in the Nu_{avg} in case of water plug; these are absent in the glycerin system. Both these transport features are a direct consequence of higher Prandtl number of glycerin. In the case of water, the initial climb in Nu_{avg} is attributed to the rapid motion of the cold fluid in the central core of the plug which comes in contact with the tube wall because of greater propensity of frequency of internal circulations, which are present in the water plug. Thus, Nu_{avg} reaches a maximum and then starts declining as the fluid that has previously been heated completes its circulation and again comes in the contact of the wall. The cycle keeps on repeating with decreased amplitude. After some time, an asymptotic steady-state is reached and there are no more oscillations in Nu_{avg}. As explained earlier, owing to high Pr for glycerin, such fluctuations are absent in its plug. Similar observation is also reported by Walsh et al. (2011) and Young et al. (2008) with different Prandtl number fluids. Finally it is noted that an increase of about 16% in the steady-state Nu_{avg} is observed in case of glycerin plug while for water plug, this value is approximately 33%.

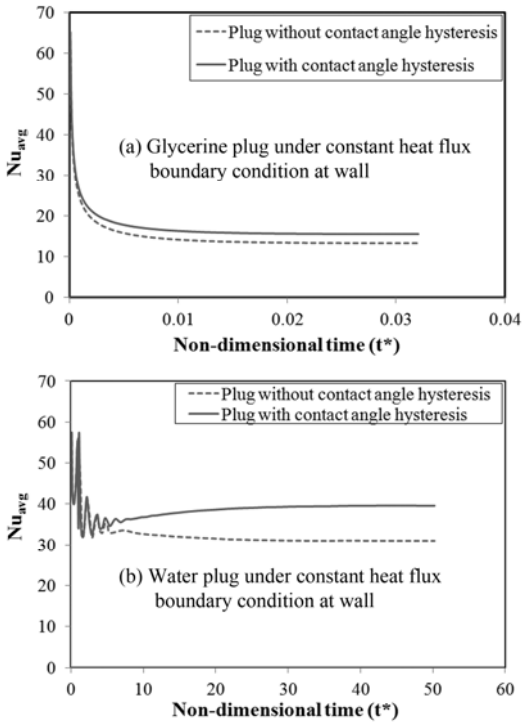

Figure 5: Average Nusselt number for (a) glycerin plug (b) water plug for L/D = 2 and $Ca = 10^{-3}$, an increase of 16% in glycerin and 33% in water is observed in case of variation in contact angle

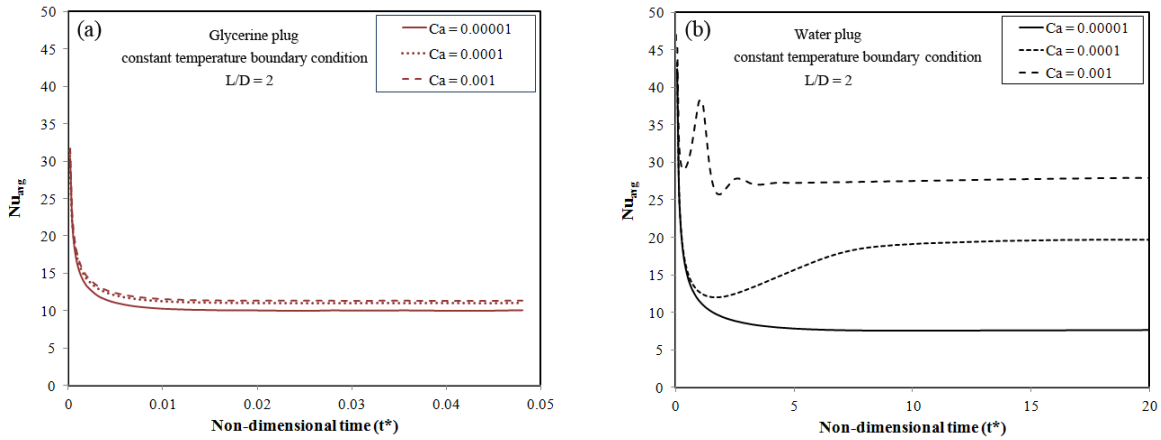

Figure 6: Temporal variation of Nu_{avg} with Ca at L/D = 2 under constant wall temperature T_w = 350 K

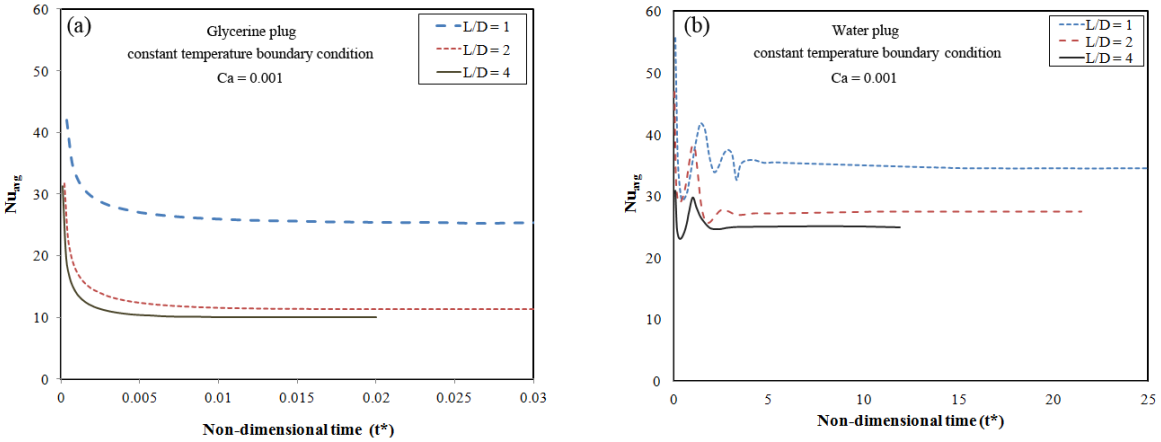

Figure 7: Temporal variation of Nu_{avg} with L/D at Ca = 0.001 under constant wall temperature T_w = 350 K

Figure 6 (a) and (b) shows the variation of Nu_{avg} with Ca, for $L/D = 2$, under constant wall temperature boundary condition. It is clear from these results that, at a constant L/D ratio, Nu_{avg} increases with Ca for both the liquids, though the increase in Nu_{avg} with Ca is more in water compared to that of glycerin. Because of high momentum diffusivity, there is no significant effect of increased velocity in case of glycerin and convection is more or less not much effected. In case of water, increase in Ca, and thus velocity has significant impact on Nu_{avg} and around 50% increment is observed. Thus, Ca plays an important role in determining the effective heat transfer coefficient in case of low Prandtl number fluids.

Figure 7 (a) and (b) shows variation of Nu_{avg} with L/D ratio at $Ca = 0.001$ for glycerin and water plug, respectively, under constant wall temperature case. Most important feature to be noted from the graph is that the heat transfer coefficient increases as the length of the plug decreases (we have not checked whether this is monotonous). Higher heat transfer coefficient in case of low L/D is because of the decrease in recirculation time scale (amount of time required for a typical fluid element to circulate once in the liquid plug) because of which relatively cooler fluid from inside the droplet core is able to reach the walls at a faster rate. Another fact which needs attention is the fact that, for any given Ca, there will be reduced oscillations of Nu_{avg} as L/D increases. Alternately, for any given L/D, reducing Ca will eventually reduce oscillations. In fact, when the cooler liquid travels a few times of its plug length, the peak, and thus amplitude of Nu_{avg} oscillations, gets reduced.

5. CONCLUSIONS

Transport parameters of isolated single liquid plugs moving inside dry capillary tubes is analyzed. It is important to include the variations in the dynamic contact angles while determining the heat transfer coefficient in isolated Taylor slug flows. Contact angle hysteresis plays a critical role in local transport behavior of liquid plugs. Furthermore, effect of Ca and L/D ratio of the plug is investigated and it is observed that high velocity (high Ca) and low L/D ratio results in significant higher heat transfer coefficients than Poiseuille flow. Together, Ca, L/D, Pr and hysteresis are the governing parameters of system transport.

NOMENCLATURE

Bo	Bond number ($Dg(\rho_l-\rho_v)/\sigma)^{0.5}$
Ca	Capillary number (-)
D	diameter of the plug (m)
g	acceleration due to gravity (m/s^2)
h	heat transfer coefficient (W/m^{2}K)
k	thermal conductivity of fluid (W/mK)
L	length of the liquid plug (m)
Nu	Nusselt number (-)
Pr	Prandtl number (-)
q''	heat flux (W)
T	temperature (^{o}C or K)
t	time (s)
t^*	non-dimensional time ($tU/(D+2L_s)$)
U	mean velocity of liquid plug (m/s)

Greek Symbols

μ	dynamic viscosity of liquid (Pa-s)
ρ	density of fluid (kg/m^3)
σ	surface tension (N/m)
θ	contact angle (rad)

Subscripts

a	advancing
d	dynamic
m, avg	Mean/ average
r	receding
s	static
w	wall
l	liquid
v	vapor

ACKNOWLEDGEMENTS

Financial support from Indo-French Center for Promotion of Advanced Research (IFCPAR) is gratefully acknowledged.

REFERENCES

Ansys Fluent® 12.0 manual

Barajas, A.M. and Panton, R.L. (1992), *The effect of contact angle on two phase flow in capillary tubes,* Int. J. Multiphase Flow 19 (2) , p. 337-346

Berthier J. (2008) *Microdrops and Digital Microfluidics,* William Andrew, NY USA

Blake, T. (2006) *The physics of moving wetting lines,* J. Colloid Interf. Sc. 299 (2006), p. 1-13

Fermigier, M., Jenffer, P. (1991) *An experimental investigation of the dynamic contact angle in liquid-liquid systems,* J. Colloid Interface Sc. 146(1), p. 226-241

Gunther, A., Khan, S.A., Thalmann, M., Trachsel, F., Jensen, K.F. (2004) *Transport and reaction in microscale segmented gas-liquid flow* Lab on a Chip 4, p. 278-286

Hoffman, R. (1974) *A study of advancing interface*, J. Colloid Interface Sc. 50(2), p. 228-241

Kolb, W.B., Cerro, R.L.(1991) *Coating the inside of a capillary of square cross section,* Chem. Engg. Sc. 46(9), p. 2181-2195

Khandekar, S., Panigrahi, P.K., Lefevre, F., Bonjour, J. (2010) *Local hydrodynamics of flow in a pulsating heat pipe: a review,* Frontiers in Heat Pipes 1, 023003 (2010)

Lee and Lee (2008) *Pressure drop of two-phase plug flow in round mini-channels: Influence of surface wettability,* Exp. Thermal Fluid Science 32 (2008), p. 1716-1722

Rose, W., Heins, R.W. (1962) *Moving interfaces and contact angle rate-dependency,* J. Colloid Science 17(1), p. 39-48

Rosengarten, G., Cooper-White, J., Metcalfe, G. (2006) *Experimental and analytical study of the effect of contact angle on liquid convective heat transfer in micro channels,* Int. J. Heat Mass Transf. 49(2006), p. 4161-4170

Shekhavat, S., Khandekar, S., Panigrahi, P.K. *Hydrodynamic study of an oscillating meniscus in a square mini-Channel,* Proc. Micro/Nano-scale Heat Mass Transf. Int. Conf., Shanghai, China

Tripathi, A., Khandekar, S., Panigrahi, P.K. (2010) *Oscillatory contact line motion inside capillaries,* Proc. 15th Int. Heat Pipe Conf., Clemson, USA

Triplett, K.A., Ghiaasiaan, S.M., Abdel-Khalik, S.I., Sadowski, D.L. (1999) *Gas-liquid two-phase flow in micro channels*, Int. J. Multiphase Flow 25(3), p. 377-394

Walsh, P.A., Walsh, E.J. and Muzychka, Y.S. (2011) *Prandtl and capillary effects on heat transfer performance within laminar liquid-gas slug flows,* Int. J. of Heat Mass Transf. 54(2011), p. 4752-4761

Young, P. and Mohseni, K. (2008) *The effect of droplet length on Nusselt numbers in digitized heat transfer,* IEEE 978-1-4244, p 1701-1708

Zheng, Y. Fujioka, H. Grotberg, J.B. (2007) *Effect of gravity, inertia and surfactant on steady plug propagation in a two dimensional channel*, Phy. Fluids 19, p. 082107-1-082107-16

Zhao, T.S., Bi, Q.C. (2001) *Co-current air water two phase flow patterns in vertical triangular micro channels*, Int. J. Multiphase Flow 27(5), p.765-782